Magnetorheological Fluid-Based Flow Control for Soft Robots

*Kevin McDonald, Abigail Rendos, Stephanie Woodman, Keith A. Brown, and Tommaso Ranzani**

Fluidic soft robots bring a high degree of dexterity and adaptability to robotics problems requiring safe interactions with complex structures. While they are low cost and easy to manufacture, they are difficult to control due to their typical reliance on external pressure sources that become bulky as more degrees of freedom are introduced to the robot. Various techniques from microfluidics and fluid logic are used to introduce valves into soft robots to increase their autonomy, although this has frequently introduced unwanted rigidity. Herein, a magnetorheological (MR) fluid valve that uses magnetic fields to control the pressure within a continuous-flow fluidic actuator is introduced. A predictive model for the pressure drop in such a flow is presented and validated experimentally. Guidelines for the design of single- and multiactuator systems with a single inlet and outlet are presented. The introduction of actuation methods that simplify fluidic control via the application of magnetic fields leads to robots capable of increased autonomy in a scalable and compliant format.

Soft robots are uniquely suited to solving many of the most complex, sensitive problems facing the robotics community.[1] With distributed degrees of freedom (DoF) and compliant structures, they can operate with motions and in locations that are unavailable to their traditional rigid counterparts.[2,3] Even a simple, low-cost soft robot can have a high degree of dexterity, adaptability, and redundancy, allowing for safe interaction with a variety of environments and biological structures.[4–6] While a variety of actuation methods have been explored, such as shape-memory alloys,[7,8] dielectric elastomers,[9] ionic polymers,[10,11] and hydrogel-based actuators,[12–14] among others, fluid-powered soft robots remain the most widespread due to their capacity to deliver large forces, large strokes, ease of fabrication, low cost, and safety.[4,15] In these systems, a fluid (liquid or gas) is used to pressurize a soft structure in a controllable way. Often, soft robot motion is achieved by embedding inflatable chambers within the elastomeric device and by exploiting the geometry or the mechanical properties of the materials comprising the structure such that controllable deformation can be obtained upon pressurization.[16] Previous work has demonstrated complex multi-DoF platforms achievable via progress in the manufacturing of soft structures.[17–22]

However, as scientists and engineers continue to develop innovative systems that push the boundaries of dexterity and miniaturization, existing soft robots' limitations become apparent by way of several unsolved challenges related to controlling such complexities. Primarily, current fluidic-powered soft robots require one individually controlled fluidic line for each DoF, leading to various fundamental issues, including 1) how to individually control a large number of lines, 2) the limitations on the robot scale induced by the physical dimensions and quantity of external fluidic connections for a given number of DoFs, 3) the inability of the fixed fluidic network within the soft robot to adapt to the robot's changing needs, and 4) the need for tubing tethered to external flow control elements that together limit the independence and motility of the robot. While the limitations to mobility that a tether of tubes introduces to a soft robot are evident, the tubing itself also introduces a number of complications to the robot's dynamics and overall design. Large lengths of tubing between the robot and its pressure source may allow it to operate more remotely but introduce a control delay due to resistance proportional to the tube's length. Such delays reduce the speed of the robot, whereas the losses similarly reduce efficiency. While stiffer tubing can mitigate such effects, it limits the intrinsic advantages of soft robots and alters the delicate

K. McDonald, S. Woodman, Prof. K. A. Brown, Prof. T. Ranzani
Department of Mechanical Engineering
Boston University
Boston, MA 02215, USA
E-mail: tranzani@bu.edu

A. Rendos, Prof. K. A. Brown, Prof. T. Ranzani
Division of Materials Science and Engineering
Boston University
Boston, MA 02215, USA

Prof. T. Ranzani
Department of Biomedical Engineering
Boston University
Boston, MA 02215, USA

Prof. K. A. Brown
Department of Physics
Boston University
Boston, MA 02215, USA

mechanics of the system. In addition, the volume occupied by these tubes can be a limiting factor in scaling down soft robots, especially as the actuators themselves approach the micron scale.[6] These design issues remain a barrier to the use of soft robots as tools for applications that require time-sensitive, precision maneuvers in delicate environments, such as medical procedures and exploration.

A number of advancements have been made to increase the autonomy of fluidic soft robots.[23] These can be broadly classified into two categories: 1) integrating the supply of pneumatic or hydraulic power within the robot and 2) introducing logic to control the application of an external power source. Integrated soft robot pressure supply technologies primarily rely on combustion or other chemical processes which introduce challenges when trying to accurately control multiple DoFs.[24,25] By contrast, integrating fluid logic into a soft robot can preserve the control of many DoFs at the expense of requiring an external connection to a pressure controller, albeit with fewer tubes when compared with a similar robot without integrated fluid logic.[26,27] This paper focuses on the integration of such on-board fluid-processing capabilities.

The development of fluid logic for soft robots has largely focused on novel techniques for constructing soft, flexible valves. A soft, pressure-activated valve for the control of a catheter is presented in a previous study.[28] However this valve can only control a single actuator and only within a specific range of pressures. In microfluidics, progress has been made toward controlling multiple fluidic lines by creating control systems analogous to those in electronics.[29–33] Such techniques have been implemented into easily miniaturized devices capable of increased autonomy relative to typical fluidic soft robots.[34] However, this has been done at the expense of introducing significant rigidity into the system by way of large thickness or the introduction of stiff materials.[35] Furthermore, such systems still require multiple fluidic input control lines.[36] Actively controlled systems have been developed in which entirely mechanical robots can be constructed using bistable soft valves that exploit differential pressures and hysteresis to systematically control airflow in two tubes.[37] Such valves have furthermore been used to implement digital logic functions including oscillation and memory.[38–40] A different valve has been implemented using electropermanent magnets and short electrical pulses to control soft robot locomotion.[41] Some degree of innate intelligence can also be provided to a robot by exploiting the properties of its constituent materials and structures. Possibilities include controlling the viscous dynamics within the working fluid of an actuator with asymmetrically distributed channels to generate different time-dependent deformation modes via a single pressure source.[42] Similarly, in a previous study,[43] the authors controlled the actuation sequence of a robot using the dynamics of its working fluid. Control via flow properties has the potential benefit of reducing the number of inputs into the soft robot without introducing any additional stiffness.

Smart fluids have also increasingly been used to control soft actuators. A number of devices have used electrorheological (ER) fluids which solidify in the presence of strong electric fields.[44,45] These fluids have been used to create fully soft valves which can be used to control several actuators simultaneously or integrate into a single microscale actuator.[46,47] While these devices can be very power efficient, they require kilovolt potentials to function.[46] Magnetorheological (MR) fluids are a similar class of materials that respond to magnetic fields. These fluids typically consist of micron-size ferrous particles in a carrier fluid such as oil or water. In the presence of a magnetic field, these particles align and cause the fluid to exhibit a yield stress that increases with field.[48] Compared with ER fluids, electromagnetically controlled MR fluids require higher power but much lower voltages to operate. MR fluids may be promising for use in larger robots where greater forces have to be applied due to the fluid's ability to achieve much higher yield stresses.[49] MR fluids have long been used in commercial applications for adaptive damping systems,[50] but recently their controllable yield stress has begun to be investigated for use in soft robotics. Several groups have explored mixing MR fluids with silicone to create magnetorheological elastomers (MREs). These have then been used to create structures with shape-memory behaviors and selective stiffening.[51] MR fluids and elastomers have been successfully used to power both rigid and flexible micropumps, respectively.[52,53] Magnetic fluids have been introduced to soft robots to provide locomotion but only as a means to make the entire structure magnetic and not in a manner that exploits the MR effect on yield stress.[54] Incorporating MR fluids into a soft robot in a tunable manner remains a challenge, whose solution would provide the possibility to exploit the same fluid used for actuation, to embed flow control components on board the robot.

In this paper, we present a platform for controlling soft robotic devices using MR fluid as the working fluid. In this way, the application of a magnetic field directly affects the pressure drop across a given region in the flow, which allows for the integration of flow control components, such as valves on-board (**Figure 1**). We investigate how MR fluids can be used to selectively control multi-DoF fluidic soft robots (Figure 1a). Specifically, given the fact that fluidic actuation is caused by a pressure gradient, we characterize the possibility of generating such gradients via applied magnetic fields (Figure 1b). We adopted well-established actuator designs[55–59] to validate the functionality of the proposed MR fluid-based flow control paradigm.

While it is necessary to provide a return channel to allow the MR fluid to circulate throughout the device, Figure 1a shows that it is still possible to actuate a closed channel connected as a branch off from the path of circulation (i.e., the legs and gripper for a multi-DoF soft robot based on a previous study[59]). However, the two circulation channels (i.e., the inlet and outlet) are the only tubes needed for any given robot with an arbitrary number of independent actuators. A strategically placed magnetic field can then be used to modulate the pressure of the flow to inflate soft actuators. Such a field can be generated either using movable permanent magnets or embedding electromagnets in the structure. If electromagnets are used, the fluid's yield stress can be directly controlled via an applied voltage.

Figure 1b shows how the MR fluid can be used to control the pressure in a continuously flowing channel and a connected soft actuator. The application of a magnetic field causes the suspended ferrous particles in the MR fluid to align to such a field. This results in an increase in pressure between the source and the location where the magnetic field is applied, causing the motion of the actuator. Figure 1c (left) shows the positioning of the fields in one of the concept robot's MR fluid valves
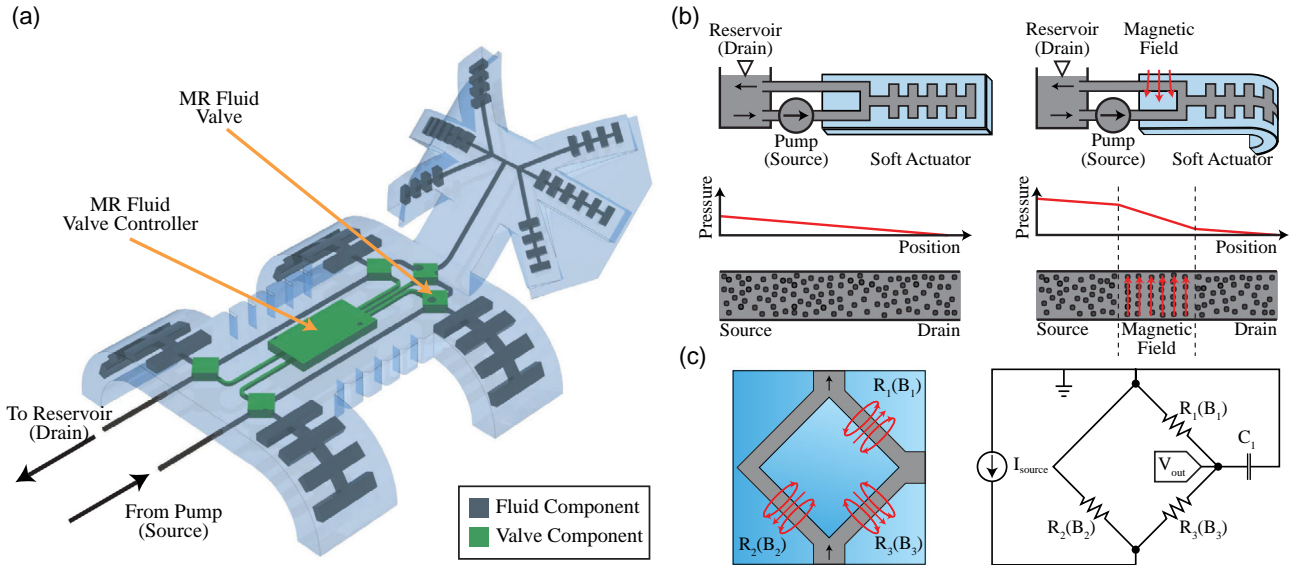
Figure 1. a) A multi-DoF soft robot concept with integrated MR fluid valves. b) (Left) Soft actuator showing pressure and recirculating MR fluid behavior in the absence of a magnetic field. (Right) Soft actuator showing pressure and MR fluid behavior in the presence of a magnetic field. c) (Left) Scheme of the MR fluid valve indicated in (a). Locations of the applied magnetic fields necessary to provide control to one of the robot's right legs: fields B_1 and B_2 are used to control the pressure inside the actuator, whereas field B_3 can be used to cut off flow from the actuator entirely. (Right) A circuit schematic analogous to the fluid circuit on the left where increasing the values of R_1 and R_2 (which are dependent on magnetic field B_1 and B_2, respectively) increase the voltage output, V_{out}. I_{source} is analogous to the flow rate at the pump. C_1 is analogous to the actuator itself.

(Figure 1a). The field B_1 acts as a variable resistor and directly increases the pressure in the valve's associated actuator. Field B_2 is applied simultaneously to B_1 such that both branches have similar resistances, which are necessary to prevent the flow from simply bypassing the actuator. Field B_3 serves as an on/off valve and can be applied to force the flow to bypass the actuator entirely, thus representing how the individual control of each of the robot's legs of Figure 1a could be achieved.

Under laminar flow conditions, this may be thought of as analogous to the electrical circuit shown in Figure 1c (right), where the magnetic fields control the values of the channel resistances and the soft actuator may be modeled as a capacitor, with voltage mapping to pressure and the flow rate at the pump being represented by I_{source}. Increasing the values of resistors R_1 and R_2 increases the output voltage, V_{out}, thus modeling the inflation of the actuator (modeled as a capacitor C_1). For sufficiently large values of R_3, V_{out} will be negligible, and the flow (i.e., the current) will thus go through R_2 without charging C_1, representing the fact that the actuator will not inflate. For an ideal DC current, V_{out} is given by

$$V_{out} = \left(\frac{R_1(B_1) \times R_2(B_2)}{R_1(B_1) + R_2(B_2) + R_3(B_3)} \right) \times I_{source} \qquad (1)$$

A model for predicting the pressure drop of the MR fluid in the vicinity of a magnetic field of a known strength has been developed using the Bingham plastic fluid model and the Buckingham Reiner equation for axial flow in a circular tube.[60] The Bingham plastic constitutive equation is given by Equation (2).

$$\tau_{yx} = \tau_0(B) - \eta_0(B)\frac{dv_x}{dy} \quad \tau_{yx} \geq \tau_0(B) \qquad (2a)$$

$$\frac{dv_x}{dy} = 0 \quad \tau_{yx} \leq \tau_0(B) \qquad (2b)$$

where τ_{yx} is shear stress, τ_0 is the yield stress, η_0 is the Bingham viscosity, and v_x is velocity. For MR fluid, τ_0 and η_0 are functions of magnetic field B. The Buckingham Reiner equation is given by Equation (4).

$$Q = \frac{\pi \times \Delta P \times R^4}{8 \times \eta_0 \times L} \left[1 - \frac{4}{3}\left(\frac{2 \times \tau_0 \times L}{\Delta P \times R}\right) + \frac{1}{3}\left(\frac{2 \times \tau_0 \times L}{\Delta P \times R}\right)^4 \right] \qquad (3)$$

where Q is the flow rate, ΔP is the change in pressure over length L, and R is the radius of the tube. The values of τ_0 and μ_0 were determined for a range of magnetic fields via rheology. We manufactured a water-based MR fluid for this paper, as its viscosity was lower than commercially available oil-based MR fluids. The specific composition of the MR fluid is described in the Experimental Section.

A commercial rheometer (TA Instruments, DHR-1 with TA Instruments Magnetorheology accessory) was used in flow mode to measure stress at shearing strain rates of 20–200 s^{-1} with seven points per decade, each averaged over 30 s. These measurements were taken at logarithmically spaced values of B from 0.005 to 1 T and were fit to Equation (2) to calculate τ_0 and η_0. These results are shown in **Figure 2**a,b. Equation (4) was then solved using MATLAB to predict the pressure drop for the experimental setup detailed.

To test the efficacy of the MR fluid for use in soft robotic systems and validate the model, a series of tests were conducted.
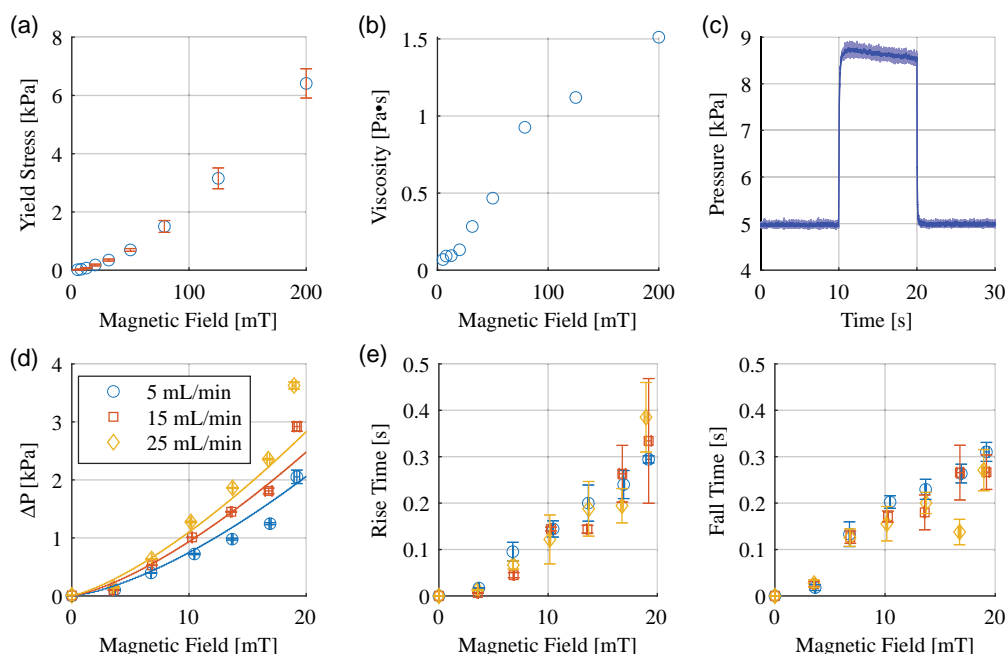
Figure 2. a) Yield stress results from rheology using Bingham plastic fit. b) Bingham viscosity results from rheology. c) Plot of pressure versus time at a flow rate of 25 mL min^{-1} and an applied magnetic field of 20 mT activated at $t = 10$ s and deactivated at $t = 20$ s. The shaded region denotes the standard deviation across three trials. d) Plot of the change in pressure versus magnetic field compiled from testing across three flow rates and seven applied magnetic fields. Each mark is the average of three trials, where the change in pressure is defined as the difference between the average pressure measured in the magnet-on and magnet-off states. Error bars represent the standard deviation. The solid lines are the theoretical values predicted using Equation (3) for each of the flow rates. e) Plots of the rise time (left) and fall time (right) versus magnetic field compiled from testing across three flow rates and seven applied magnetic fields. The rise time was calculated as the duration between the moment the magnet turned on and the moment the pressure achieved its average value in the magnet-on state. The fall time was calculated as the duration between the moment the magnet turned off and the moment the pressure achieved its average value in the magnet-off state. Each mark is the average of three trials. Error bars represent the standard deviation.

Using a syringe pump (Harvard Apparatus Pico Plus Elite), MR fluid was pumped through a 2 mm inner diameter tube into an open reservoir at a fixed flow rate of 5, 15, or 25 mL min^{-1} while the pressure was monitored using a pressure transducer (Nidec Copal Electronics P-7100-102GM5). A 5 mm-thick, 10 mm-radius electromagnet coil consisting of 400 turns of 36 gauge copper wire was affixed to the tube and currents ranging from 0 to 600 mA in increments of 100 mA were applied to modulate the fluid properties via the applied magnetic field. A gaussmeter (Lake Shore Cryotronics Model 425) was used to directly measure the applied field. The range of currents were chosen in part as a compromise between the generation of the desired fields with the magnets manufactured for the test and to avoid generating undesired heat, which led to changing resistance in the wires and thus unstable fields.

Three trials at each combination of the three flow rates and seven applied currents were conducted, and the results were analyzed in MATLAB. The specific details of the analysis are available in Supporting Information. Figure 2c shows a graph of pressure versus time at a flow rate of 25 mL min^{-1} and an applied magnetic field of 20 mT. The magnetic field was applied after 10 s from the beginning of the experiment and kept on for 10 s. Figure 2d shows the results in terms of pressure increase with magnetic field and Figure 2e shows the time required to activate and deactivate the change in pressure. Note that the change in pressure is defined as the difference in the average

pressure value in the magnet-on and magnet-off states (Figure 2c). Notably, the pressure response of the fluid was found to be repeatable among trials at any given set of parameters. On average across all combinations, the standard deviation of pressure was 0.6% of the mean pressure at the same point in time. Furthermore, the theoretical model was found to match the trend in the data, as the change in pressure increased with both increasing magnetic field, due to its effect on yield stress, and increasing flow rate, due to the associated increase in the Newtonian nature of the MR fluid's velocity profile (Figure 2d). While the response of the fluid slowed with increasing magnetic field, neither the rise time nor fall time exceeded 0.5 s in any tests (Figure 2e), which is compatible with the operative speeds on the order of seconds or minutes typical of soft fluidically actuated robots.[59,61]

As we envisage the possibility to control pressure in multiple actuators by controlling the magnetic field in each individual channel supplying them, we characterized potential limitations in the relative proximity between such channels. An experiment was developed using an electromagnet adjacent to a tube carrying MR fluid. By varying the distance between the electromagnet and the tube carrying the flowing fluid while monitoring the flow pressure, it was determined that there were no crosstalk effects at distances down to 1 cm at 0.5 A (see Supporting Information for additional details). Also, the use of electromagnets to generate the magnetic field causes a rise in the temperature.

We characterized heating generated using a thermocouple (McMaster part number 9251T94) placed within a tube at the center of an electromagnet. The temperature was monitored as the coil dissipated heat. For a current of 0.5 A, it took 200 s to reach 100 °C. This time is two orders of magnitude larger than the typical timescale for a soft robot's operation. This suggests that the MR fluid is unlikely to boil during normal robot operation. Furthermore, the silicone typically used to manufacture soft robots is rated for use up to 232 °C.[62,63] Further details on this test are available in Supporting Information.

To be able to incorporate the MR fluid into a soft actuator, it is necessary to have both an inlet and outlet tube to allow for flow throughout the system. This was demonstrated via a simple bending actuator manufactured out of two layers of silicone with the inlet and outlet connected via a loop (**Figure 3**a). This and all subsequent actuators were manufactured using two materials with different stiffnesses, such that when inflated the actuator would bend toward the stiffer side. With the application of a magnetic field just downstream of the actuator itself, the actuator bent as designed (Figure 3a, Movie S1, Supporting Information).

This concept was then extended by coupling three actuators together to form a soft gripper (Figure 3b). Here, the actuators were joined to a single point on the loop connecting the inlet and outlet such that all three actuators bent simultaneously when the magnetic field was applied downstream. Movie S2, Supporting Information, demonstrates the gripper grasping a plastic cup. For these tests, a grade N35SH permanent disk magnet with a diameter of 12.5 mm and thickness of 12.5 mm (McMaster part number 5862K29) was used. With the magnet at a distance of 15 mm from the surface of the robot, the field experienced by the fluid was ≈33 mT.[64] MR fluid flow was provided continuously by a peristaltic pump (Fisherbrand GP1000) operating at 30 rpm.

To demonstrate the possibility to control multiple actuators independently using the MR fluid, two bending actuators were fabricated in a parallel configuration as a single device such that they shared a common inlet and outlet to guarantee the continuous flow of the fluid (Figure 3c,d). Via the application of strategically placed magnets (McMaster part number 5862K985), any combination of the two actuators' bending states can be achieved.
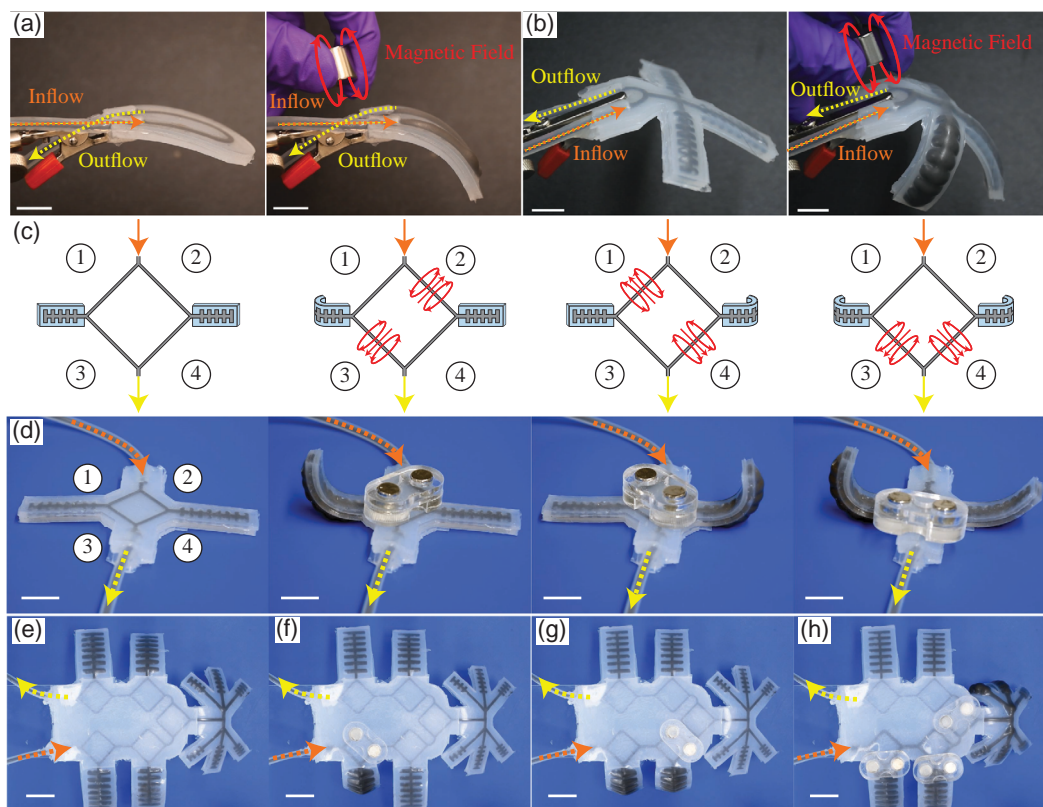
Figure 3. a) Soft actuator constructed as a looped channel with continuously flowing MR fluid before and after application of a downstream magnetic field. Scale bars represent 1 cm. b) Soft gripper comprising three coupled actuators before and after the application of a magnetic field downstream. Scale bars represent 1 cm. c) Schematic showing magnetic field placement to independently control the motion of two actuators (shown in d); the MR fluid is continuously flowing from the top (orange arrow). In the left image, no fields are applied resulting in no actuation. In the middle left image, the field at point 3 inflates the left actuator whereas the field at point 2 blocks the pressure from dissipating through the right actuator. In the middle right image, the field at point 4 inflates the right actuator whereas the field at point 1 blocks the pressure from dissipating through the left actuator. In the right image, the fields at points 3 and 4 inflate both the left and right actuators, respectively. d) The experimental images corresponding to the schematic in (c). The two permanent magnets are held at a fixed distance from each other by an acrylic fixture. Scale bars represent 1 cm. e) Demonstration of selective actuation of a five DoF soft robot with continuously recirculating MR fluid. Here, the robot is seen with no DoFs actuated. Scale bar represents 2 cm. f) The robot with one leg leg actuated. g) The robot with two legs actuated. h) The robot with its gripper actuated and neither of the two upstream legs actuated.

**ADVANCED
SCIENCE NEWS**
www.advancedsciencenews.com

**ADVANCED
INTELLIGENT
SYSTEMS**
Open Access
www.advintellsyst.com

Figure 3c,d shows these logical states schematically and the results of experiments corresponding to each, respectively. In the first state, the MR fluid flows continuously without causing actuation to either side. In the second state, magnetic fields are applied at points 2 and 3, inflating only the left side. In the third state, fields are applied at points 1 and 4 to actuate the right side. In the final state, fields at points 3 and 4 actuate both sides. All three states with at least one actuator activated require two magnetic fields. The volumetric flow rate of the flowing fluid was not altered in between the four states, and the magnetic fields were the only applied stimuli. The discrepancy in the amount of inflation of the right-side actuator between the middle right image in Figure 3d, where it alone is inflated, and the right-most image in Figure 3d, where the left side is also actuated, is caused by manufacturing inconsistencies. Due to a small difference in the thickness of the silicone membrane, which inflates to bend the actuator, the two sides on the device tend to inflate by a different amount for the same applied pressure.

The behavior of the two independent actuators shown in Figure 3d was extended to a robot based on the concept shown in Figure 1a. This robot has five DoFs: four independent legs and a gripper consisting of six coupled actuators. Each DoF is connected to its own logic node (Figure 1c) identical to the one at the center of device, as shown in Figure 3c,d, with the exception that only the one actuator is connected. Any combination of the five DoFs can be achieved using magnetic fields as before. It is important to note that as the nodes are connected in series between the inlet and the outlet, without intervention, inflating one actuator will also inflate all the actuator upstream from that point. However, the magnetic fields may be placed on the upstream actuators such that they are bypassed by the flow, preventing inflation. The simultaneous inflation of multiple actuators may also be exploited if desired. Figure 3e shows the robot with no DoFs actuated and the MR fluid continuously recirculating. Figure 3f shows the robot with one DoF actuated. Figure 3g shows the robot with two DoFs actuated. Figure 3h shows the robot with its gripper inflated but neither of the two upstream legs actuated. A video of this robot demonstrating the logical states is available in Movie S3, Supporting Information. This robot is intended for demonstration of the MR fluid control only, the MR fluid continuously recirculated during the experiment at a constant flow rate and the magnetic field was the only stimulus applied.

These experiments demonstrate the feasibility of the MR fluid to operate within a soft robot with branching fluid paths as both a valve to control the pressure of the flow and thus the bending of a soft fluidic actuator, as well as a switch to prevent the flow of fluid through any given path. The only difference between the two modes is the placement of the magnetic field. A magnetic field placed downstream of an actuator modulates its bending via pressure, whereas a magnetic field placed upstream of an actuator prevents flow from proceeding down that path in favor of a different path with less resistance. The fluid pressure in any given channel is therefore dependent on any magnetic fields across all the channels. Precise control of the bending of any given actuator would require fine control of the magnetic field, a task that would best be handled via electromagnets controlled via software. Actuators with integrated electromagnets present issues with regard to the production of strong fields; however,

several methods could be used to mitigate this including 1) smaller fluid channels, thereby requiring lower fields to produce the same change in pressure, 2) a magnetic core could be added to the electromagnets, increasing the magnetic field produced at a given current by several orders of magnitude, or 3) a lower-resistance wire, such that less power would be dissipated at a given current. Alternatively, various projects have investigated the use of external magnetic fields as a means of precisely controlling the navigation of a robot with a ferrous element through a complex environment, such as in endoscopy.[65–70] This has proven to be a promising technique for the control of microrobots.[71,72] Similar techniques could be applied to control MR fluid components.

In this paper, MR fluid has been explored as a means to create on-board flow control components in soft robotic systems. By applying a magnetic field to a continuously flowing MR fluid, the fluid's material properties were modulated, increasing the pressure gradient in the flow and activating actuators. A new design methodology was introduced in which a single recirculating channel with one inlet and one outlet could be used to pressurize multiple classes of devices: 1) individual actuators (Figure 3a), 2) coupled actuators (Figure 3b), and 3) systems with multiple independently controlled actuators (Figure 3d–h). Introducing additional complexity did not require any additional tubing. In this way, the addition of subsequent actuators to a soft robot requires no additional fluidic lines to provide control. Magnetic fields were generated both by permanent magnets and by electromagnets. With a remotely controlled electromagnet, the MR fluid's pressure response was controlled in a repeatable manner. Furthermore, the fluid responds with sub-second times that compare favorably with existing soft robots that frequently exhibit locomotion on the order of seconds.[59,73] These results, along with the negligible influence of crosstalk on the systems tested, give credence to the continued development of MR fluids as a means to integrate on-board fluidic control via magnetic fields into soft robotics. This technology promises to reduce the reliance on bulky fluidic connections by shifting control to the scalable and easily implemented electromagnetic domain. Embedding MR fluid and electromagnets onto soft robots will provide a pathway toward untethered, autonomous soft systems capable of complex motions and behaviors. This promises to drive the development of practical devices for applications from medical robotics to the exploration of complex terrains for search and rescue. In future work, the authors plan to exploit improvements to the composition of the MR fluid which can produce materials that achieve higher yield stresses at lower magnetic fields.[74]

Experimental Section

Soft actuators were molded layerwise. 1.6 mm-thick acrylic sheets were laser cut and assembled into molds using acrylic cement. Ecoflex 00-30 (Smooth on, Macungie, PA, USA) and Dragon Skin 20 (Smooth on, Macungie, PA, USA) were mixed with a planetary mixer and poured into the molds such that the Ecoflex contained the fluid channels and the Dragon Skin provided a strain-limiting layer. The filled molds were degassed at 90 kPa for 5 min and cured in a 70 °C oven for 30 min. The Dragon Skin layer was then spin coated with a 300 µm layer of Ecoflex 00-30. The two molded layers were then placed in contact and cured at 70 °C for an additional 30 min to bond together.

**ADVANCED
SCIENCE NEWS**

www.advancedsciencenews.com

**ADVANCED
INTELLIGENT
SYSTEMS**
Open Access

www.advintellsyst.com

Silicone tubing with an inner diameter of 1.6 mm and an outer diameter of 3.2 mm was then inserted into the structure and sealed with more Ecoflex 00-30 then cured. The MR fluid consisted of 23% carbonyl iron particles (3–5 μm size, Skyspring Nanomaterials, 0990JH) by volume, 75% deionized water by volume, and 2% xanthan gum (Sigma Aldrich, G1253) by volume, vortexed to form a homogeneous mixture. Xanthan gum was used as a thixotropic agent to reduce the sedimentation of the iron particles and aided in the stability of the fluid.

Supporting Information

Supporting Information is available from the Wiley Online Library or from the author.

Conflict of Interest

The authors declare no conflict of interest.

[1] G. M. Whitesides, *Angew. Chem. Int. Ed.* **2018**, *57*, 4258.
[2] C. Laschi, B. Mazzolai, M. Cianchetti, *Sci. Robot.* **2016**, *1*, eaah3690.
[3] D. Rus, M. T. Tolley, *Nature* **2015**, *521*, 467.
[4] P. Polygerinos, N. Correll, S. A. Morin, B. Mosadegh, C. D. Onal, K. Petersen, M. Cianchetti, M. T. Tolley, R. F. Shepherd, *Adv. Eng. Mater.* **2017**, *19*, 12.
[5] K. C. Galloway, K. P. Becker, B. Phillips, J. Kirby, S. Licht, D. Tchernov, R. J. Wood, D. F. Gruber, *Soft Robot.* **2016**, *3*, 23.
[6] M. Cianchetti, C. Laschi, A. Menciassi, P. Dario, *Nat. Rev. Mater.* **2018**, *3*, 143.
[7] H. Rodrigue, W. Wang, M. W. Han, T. J. Kim, S. H. Ahn, *Soft Robot.* **2017**, *4*, 3.
[8] J. K. Paik, E. Hawkes, R. J. Wood, *Smart Mater. Struct.* **2010**, *19*, 12.
[9] S. Shian, K. Bertoldi, D. R. Clarke, *Adv. Mater.* **2015**, *27*, 6814.
[10] Y. Bahramzadeh, M. Shahinpoor, *Soft Robot.* **2014**, *1*, 38.
[11] S. Sareh, J. Rossiter, *Smart Mater. Struct.* **2013**, *22*, 014004.
[12] H. Banerjee, M. Suhail, H. Ren, *Biomimetics* **2018**, *3*, 15.
[13] H. Yuk, S. Lin, C. Ma, M. Takaffoli, N. X. Fang, X. Zhao, *Nat. Commun.* **2017**, *8*, 14230.
[14] X. Le, W. Lu, J. Zhang, T. Chen, *Adv. Sci.* **2019**, *6*, 1801584
[15] M. Cianchetti, T. Ranzani, G. Gerboni, T. Nanayakkara, K. Althoefer, P. Dasgupta, A. Menciassi, *Soft Robot.* **2014**, *1*, 122.
[16] B. Gorissen, D. Reynaerts, S. Konishi, K. Yoshida, J. W. Kim, M. De Volder, *Adv. Mater.* **2017**, *29*, 1604977.
[17] R. F. Shepherd, F. Ilievski, W. Choi, S. A. Morin, A. A. Stokes, A. D. Mazzeo, X. Chen, M. Wang, G. M. Whitesides, *Proc. Natil Acad. Sci.* **2011**, *108*, 20400.
[18] P. H. Nguyen, C. Sparks, S. G. Nuthi, N. M. Vale, P. Polygerinos, *Soft Robot.* **2019**, *6*, 38.
[19] T. Ranzani, G. Gerboni, M. Cianchetti, A. Menciassi, *Bioinspir. Biomimet.* **2015**, *10*, 3.
[20] A. D. Marchese, R. Tedrake, D. Rus, *Int. J. Robot. Res.* **2016**, *35*, 1000.
[21] T. Ranzani, S. Russo, N. W. Bartlett, M. Wehner, R. J. Wood, *Adv. Mater.* **2018**, *1802739*, 1802739.
[22] S. T. Mahon, J. O. Roberts, M. E. Sayed, D. H. T. Chun, S. Aracri, R. M. McKenzie, M. P. Nemitz, A. A. Stokes, *Biomimetics* **2018**, *3*, 3.
[23] S. I. Rich, R. J. Wood, C. Majidi, *Nat. Electron.* **2018**, *1*, 102.
[24] R. F. Shepherd, A. A. Stokes, J. Freake, J. Barber, P. W. Snyder, A. D. Mazzeo, L. Cademartiri, S. A. Morin, G. M. Whitesides, *Angew. Chem. Int. Ed.* **2013**, *52*, 2892.
[25] M. T. Tolley, R. F. Shepherd, M. Karpelson, N. W. Bartlett, K. C. Galloway, M. Wehner, R. Nunes, G. M. Whitesides, R. J. Wood, in *IEEE Int. Conf. on Intelligent Robots and Systems*, IEEE, Piscataway, NJ **2014**, pp. 561–566.
[26] J. W. Booth, J. C. Case, E. L. White, D. S. Shah, R. Kramer-Bottiglio, in *IEEE Int. Conf. on Soft Robotics, RoboSoft*, IEEE, Piscataway, NJ **2018**, pp. 25–30.
[27] G. Gerboni, T. Ranzani, A. Diodato, G. Ciuti, M. Cianchetti, A. Menciassi, *Meccanica* **2015**, *50*, 2865.
[28] K. Ikuta, Y. Matsuda, D. Yajima, Y. Ota, *IEEE/ASME Trans. Mechatron.* **2012**, *17*, 876.
[29] Q. Zhang, M. Zhang, L. Djeghlaf, J. Bataille, J. Gamby, A. M. Haghiri-Gosnet, A. Pallandre, *Electrophoresis* **2017**, *38*, 953.
[30] F. G. Woodhouse, J. Dunkel, *Nat. Commun.* **2017**, *8*, 15169.
[31] A. Ainla, M. M. Hamedi, F. Güder, G. M. Whitesides, *Adv. Mater.* **2017**, *29*, 38.
[32] J. A. Weaver, J. Melin, D. Stark, S. R. Quake, M. A. Horowitz, *Nat. Phys.* **2010**, *6*, 218.
[33] M. A. Unger, H. P. Chou, T. Thorsen, A. Scherer, S. R. Quake, *Science* **2000**, *288*, 113.
[34] S. T. Mahon, A. Buchoux, M. E. Sayed, L. Teng, A. A. Stokes, in *RoboSoft 2019–2019 IEEE Int. Conf. on Soft Robotics*, IEEE, Piscataway, NJ **2019**, pp. 782–787.
[35] M. Wehner, R. L. Truby, D. J. Fitzgerald, B. Mosadegh, G. M. Whitesides, J. A. Lewis, R. J. Wood, *Nature* **2016**, *536*, 451.
[36] N. W. Bartlett, K. P. Becker, R. J. Wood, *Soft Matter.* **2020**.
[37] P. Rothemund, A. Ainla, L. Belding, D. J. Preston, S. Kurihara, Z. Suo, G. M. Whitesides, *Sci. Robot.* **2018**, *3*, eaar7986.
[38] D. J. Preston, P. Rothemund, H. J. Jiang, M. P. Nemitz, J. Rawson, Z. Suo, G. M. Whitesides, *Proc. Natl. Acad. Sci.* **2019**, *116*, 7750.
[39] D. J. Preston, H. J. Jiang, V. Sanchez, P. Rothemund, J. Rawson, M. P. Nemitz, W.-K. Lee, Z. Suo, C. J. Walsh, G. M. Whitesides, *Sci. Robot.* **2019**, *4*, eaaw5496.
[40] M. P. Nemitz, C. K. Abrahamsson, L. Wille, A. A. Stokes, D. J. Preston, G. M. Whitesides, in *IEEE Int. Conf. on Soft Robotics 2020*, IEEE, Piscataway, NJ **2020**.
[41] A. D. Marchese, C. D. Onal, D. Rus, in *IEEE Int. Conf. on Intelligent Robots and Systems*, IEEE, Piscataway, NJ **2011**, pp. 756–761.
[42] Y. Matia, T. Elimelech, A. D. Gat, *Soft Robot.* **2017**, *4*, 126.
[43] N. Vasios, A. J. Gross, S. Soifer, J. T. Overvelde, K. Bertoldi, *Soft Robot.* **2019**.
[44] A. Sadeghi, L. Beccai, B. Mazzolai, in *IEEE Int. Conf. on Intelligent Robots and Systems*, IEEE, Piscataway, NJ **2012**, pp. 4237–4242.
[45] A. Helal, B. Qian, G. H. McKinley, A. E. Hosoi, *Phys. Rev. Appl.* **2016**, *5*, 064011.
[46] A. Zatopa, S. Walker, Y. Menguc, *Soft Robot.* **2018**, *5*, 258.
[47] T. Sudhawiyangkul, K. Yoshida, S. I. Eom, J.-W. Kim, *Microsyst. Technol.* **2019**, *2*, 1507.
[48] S. Genc, P. Phule, *Smart Mater. Struct.* **2002**, *140*, 140.

[49] J. Carlson, D. Catanzarite, K. St. Clair, *Int. J. Modern Phys. B* **1996**, *10*, 2857.

[50] F. Gao, Y. N. Liu, W. H. Liao, in *Sensors and Smart Structures Technologies for Civil, Mechanical, and Aerospace Systems*, SPIE, Bellingham, WA **2017**, p. 101681.

[51] P. Testa, R. W. Style, J. Cui, C. Donnelly, E. Borisova, P. M. Derlet, E. R. Dufresne, L. J. Heyderman, *Adv. Mater.* **2019**, *31* 1900561.

[52] Y. Liang, *Ph.D. Thesis*, Massachusetts Institute of Technology, **2015**.

[53] M. Behrooz, F. Gordaninejad, *Smart Mater. Struct.* **2016**, *25*, 11.

[54] N. Saga, T. Nakamura, *Smart Mater. Struct.* **2004**, *13*, 566.

[55] F. Ilievski, A. D. Mazzeo, R. F. Shepherd, X. Chen, G. M. Whitesides, *Angew. Chem. Int. Ed.* **2011**, *50*, 1890.

[56] K. M. de Payrebrune, O. M. O'Reilly, *Extreme Mech. Lett.* **2016**, *8* 38.

[57] B. Mosadegh, P. Polygerinos, C. Keplinger, S. Wennstedt, R. F. Shepherd, U. Gupta, J. Shim, K. Bertoldi, C. J. Walsh, G. M. Whitesides, *Adv. Funct. Mater.* **2014**, *24*, 2163.

[58] M. T. Tolley, R. F. Shepherd, B. Mosadegh, K. C. Galloway, M. Wehner, M. Karpelson, R. J. Wood, G. M. Whitesides, *Soft Robot.* **2014**, *1*, 213.

[59] A. Yin, H. Ching Lin, J. Thelen, B. Mahner, T. Ranzani, *Adv. Intell. Syst.* **2019**, *1*, 1900089.

[60] R. B. Bird, G. C. Dai, B. J. Yarusso, *Rev. Chem. Eng.* **1983**, *1*, 1.

[61] M. Calisti, G. Picardi, C. Laschi, *J. Roy. Soc. Interface* **2017**, *14*, 130.

[62] Smooth-On, Dragon Skin 20, https://www.smooth-on.com/products/dragon-skin-20/ (accessed: June 2020).

[63] Smooth-On, Ecoflex 00-20, https://www.smooth-on.com/products/ecoflex-00-20/ (accessed: June 2020).

[64] K&J Magnetics, The K&J Magnetic Field Calculator, https://www.kjmagnetics.com/fieldcalculator.asp (accessed: June 2020).

[65] G. Ciuti, P. Valdastri, A. Menciassi, P. Dario, *Robotica* **2010**, *28*, 199.

[66] S. Yim, M. Sitti, *IEEE Trans. Robot.* **2012**, *28*, 183.

[67] E. Diller, J. Giltinan, M. Sitti, *Int. J. Robot. Res.* **2013**, *32*, 614.

[68] D. Son, H. Gilbert, M. Sitti, *Soft Robot.* **2020**, *7*, 10.

[69] Y. Kim, G. A. Parada, S. Liu, X. Zhao, *Sci. Robot.* **2019**, *4*, eaax7329.

[70] W. Hu, G. Z. Lum, M. Mastrangeli, M. Sitti, *Nature* **2018**, *554*, 81.

[71] B. E. Kratochvil, M. P. Kummer, J. J. Abbott, R. Borer, O. Ergeneman, B. J. Nelson, *IEEE Trans. Robot.* **2010**, *26*, 1006.

[72] R. S. Pierre, S. Bergbreiter, *IEEE Robot. Automat. Lett.* **2017**, *2*, 34.

[73] M. Duduta, D. R. Clarke, R. J. Wood, in *Proc. – IEEE Int. Conf. on Robotics and Automation*, IEEE, Piscataway, NJ **2017**, pp. 4346–4351.

[74] A. Rendos, S. Woodman, K. McDonald, T. Ranzani, K. A. Brown, *Smart Mater. Struct.* **2020**, *29*, 7.